Combust. Sci. and Tech., 179: 2219–2253, 2007

ISSN: 0010-2202 print/1563-521X online
DOI: 10.1080/00102200701407887

Taylor & Francis
Taylor & Francis Group

Prediction of Flame Liftoff Height of Diffusion/Partially Premixed Jet Flames and Modeling of Mild Combustion Burners

Sudarshan Kumar*
Institute of Fluid Science, Tohoku University, Sendai, Japan

P. J. Paul and H. S. Mukunda
Combustion Gasification and Propulsion Laboratory, Department of Aerospace Engineering Indian Institute of Science, Bangalore, India

Abstract: In this article, a new flame extinction model based on the k/ε turbulence time scale concept is proposed to predict the flame liftoff heights over a wide range of coflow temperature and O_2 mass fraction of the coflow. The flame is assumed to be quenched, when the fluid time scale is less than the chemical time scale (Da < 1). The chemical time scale is derived as a function of temperature, oxidizer mass fraction, fuel dilution, velocity of the jet and fuel type. The present extinction model has been tested for a variety of conditions: (a) ambient coflow conditions (1 atm and 300 K) for propane, methane and hydrogen jet flames, (b) highly preheated coflow, and (c) high temperature and low oxidizer concentration coflow. Predicted flame liftoff heights of jet diffusion and partially premixed flames are in excellent agreement with the experimental data for all the simulated conditions and fuels. It is observed that flame stabilization occurs at a point near the stoichiometric mixture fraction surface, where the local flow velocity is equal to the local flame propagation speed. The present method is used to determine the chemical time scale for the conditions existing in the mild/flameless combustion burners investigated by the authors earlier. This model has successfully predicted the initial premixing of the fuel with combustion products before the combustion reaction initiates. It has been inferred from these numerical simulations that fuel injection is followed by intense premixing with hot combustion products in the primary zone and combustion reaction follows

Received 11 May 2006; accepted 4 April 2007.
*Address correspondence to sudar4@gmail.com

further downstream. Reaction rate contours suggest that reaction takes place over a large volume and the magnitude of the combustion reaction is lower compared to the conventional combustion mode. The appearance of attached flames in the mild combustion burners at low thermal inputs is also predicted, which is due to lower average jet velocity and larger residence times in the near injection zone.

Keywords: Flame liftoff height; Mild/flameless combustion; NO_x emission

INTRODUCTION

The study of lifted flames has been an important topic of fundamental research as well as practical applications. Several of the proposed theories for the stabilization of lifted flames are reviewed and assessed by Pitts (1989, 1990), Burgess and Lawn (1999) and Upatneiks et al. (2004). The stability, liftoff mechanisms, liftoff height, liftoff velocity, blow-off velocity, flame size and pollutant emissions from turbulent jet diffusion flames have received considerable attention in recent years (Vanquickenborne and Tigglen, 1966; Burgess and Lawn, 1999; Donnerhack and Peters, 1984; Kalghatgi, 1984; Peters and Williams, 1984; Savas and Gollahalli, 1986; Pitts, 1989, 1990; Muller et al., 1994; Rokke et al., 1994; Upatneiks et al. 2004). A very brief summary of different flame liftoff theories is provided below as a backdrop for the present work, followed by the formulation of the present model, predictions of flame liftoff heights and finally modeling of flameless/mild combustion burners.

The premixed flame propagation model proposed by Vanquckenborne and Tigglen (1966) and later investigated by Kalghatgi (1984) assumes that air and fuel are completely premixed at the base of the lifted flame. According to this model, it is assumed that the turbulent flame propagation velocity s_T is equal to the flow velocity upstream of the flame front, U_{sp}. However, Pitts (1989, 1990) concluded that the premixedness model doesn't include the true physical behavior of the turbulent flow and fails to predict the correct experimental dependence of liftoff height.

Peters and Williams (1984) proposed a stabilization mechanism of lifted flames based on the laminar flamelet concept. The theory suggests that no substantial molecular premixing of fuel and air occurs for positions upstream of the combustion region. However, a recent analysis by Peters (2000) endorses the idea of flame stabilization on the basis of partially or fully premixed flame propagation analysis. The propagation speed of fully premixed turbulent flames is a function of a single parameter, namely the turbulent Damkohler number (Peters, 2000). In the

limit of $Da \rightarrow \infty$ (where $Da = s_L \ell / \ell_f u'$ is the turbulent Damkohler number), flame propagation speed becomes Damkohlar number independent. The limit $Da \rightarrow 0$ seemed to be an appropriate line of thought to explain the stabilization of lifted flames. This further leads to the derivation of the linear dependence of flame liftoff height on jet velocity and s_L^{-2}. Pitts (1989, 1990), Muller et al. (1994), and Chen and Bilger (2000) have also provided sufficient evidence of fuel and air premixing upstream of the lifted flame.

The extinction model proposed by Byggstoyl and Magnussen (1985) assumes that both fuel and air are essentially premixed at the base of the flame. According to this model, extinction occurs when this time scale matches the chemical time scale for extinction based on $C(\nu/\varepsilon)^{1/2}$ parameter. This method has been used to predict liftoff height of diluted methane flames and compared with the experimental measurements of Horch (1978). *However, the proposed $C(\nu/\varepsilon)^{1/2}$ based extinction criterion depends explicitly on the diameter of the fuel jet, a feature acknowledged by the authors themselves* (Byggstoyl and Magnussen, 1985).

The concept of triple flames has been put forward by various researchers (Ruetsch et al., 1995; Buckmaster, 1996a, 1996b; Domingo and Vervisch, 1996; Plessing et al., 1998a; Tacke et al., 1998; Chen and Bilger, 2000) to be the key to understand the stabilization of lifted flames. According to this theory, gas expansion of the premixed flame front generates a normal velocity from the stabilization point into the unburnt mixture. This leads to a diverging flow field and a lower oncoming velocity directly ahead of the triple point as shown in the studies of Chen and Bilger (2000) and Plessing et al. (1998a) and Ruetsch et al. (1995).

A detailed analysis of stabilization mechanisms of laminar lifted flames by Chen and Bilger (2000) shows that at the stabilization point, the flame propagation velocity U_p is equal to the upstream flow velocity, U_{st} along the stoichiometric mixture fraction contour. Edge flame extinction, triple flame propagation, flame front propagation and final blowout of jet diffusion flames, a function of flame liftoff height and jet velocity (jet Reynolds number) are proposed by the authors. The details of these mechanisms are shown in Figure 1.

Upatneiks et al. (2004) have carried out cinema-PIV measurements on methane jet diffusion flames in the Reynolds number range of 4300–8500. Detailed measurements of velocity, flame propagation speed, temperature and turbulence intensity suggest that edge flame extinction is the dominant mechanism for flame stabilization and that the flame is located at a radial position, outside the turbulent core jet. These measurements further show that the local flow velocities are approximately equal to the laminar flame propagation speed at the flame stabilization point and the correlation between flame propagation speed and turbulence levels is poor.

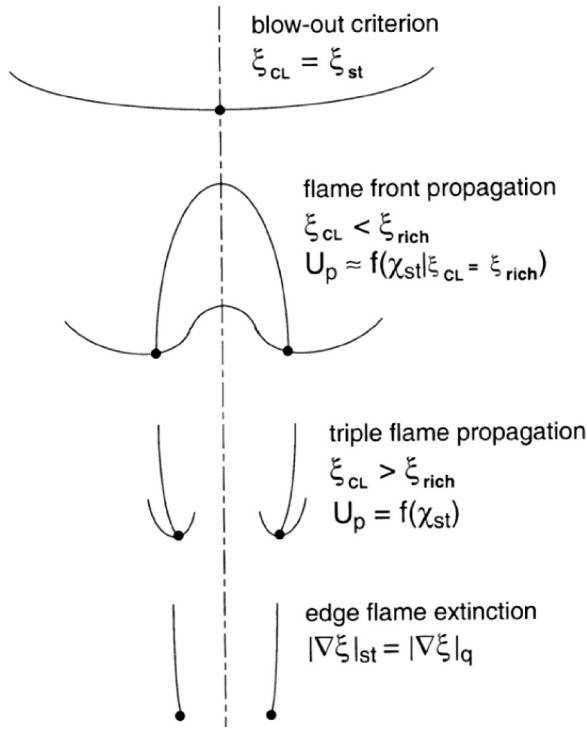

Figure 1. Schematic diagram of flame front contours and corresponding criteria for flame stability and blow-out limits for a laminar lifted flame (Chen and Bilger, 2000).

Upatneiks et al. (2004) further show that flame stabilization based on large eddy theory is also inconsistent with the experimental measurements. The experimental investigations of Starner et al. (1997) and Watson et al. (2003) show that the theory of flame quenching due to excessive scalar dissipation is inconsistent with experimental results.

Muniz and Mungal (1997) have reported PIV measurements on lifted methane and ethylene jet flames in the Reynolds number range of 3800–22000. The measurements show that the flame is located at a position where the local flow velocity is equal to flame propagation speed and does not exceed $3s_L$. These studies further show similarities between lifted flames and computed triple flames, which include divergence of streamlines near the flame stabilization point and premixed flame propagation through a fuel concentration gradient. The experimental PIV measurements on lifted methane jet flames by Schefer and Goix (1998) in the Reynolds number range of 7000–19500 show that flow velocities at the instantaneous flame stabilization point are below the expected

turbulent flame propagation speed. However a strong Reynolds number dependence on local flow velocity at the stabilization point is reported by the authors (Schefer and Goix, 1998).

They further observed that the local flow velocity at stabilization point varies from 0.2 to 1.2 times the laminar flame velocity as the Reynolds number is increased from 7000 to 19500. Therefore, the evidence provided by Schefer and Goix (1998), Muniz and Mungal (1997), Chen and Bilger (2000) and Upatneiks et al. (2004) can be interpreted as (i) edge flame extinction plays an essential role in flame stabilization at low Reynolds numbers (lower jet exit velocities) and (ii) other flame stabilization mechanisms such as turbulent premixed flame propagation plays dominant role at higher Reynolds numbers (higher jet exit velocities) (refer Figure 1) (Schefer and Goix, 1998; Chen and Bilger, 2000).

A compilation of the experimental data on flame liftoff heights from various sources is shown in Figure 2 (Horch, 1978; Donnerhack and Peters, 1984; Kalghatgi, 1984; Rokke et al., 1994). The data are plotted against non-dimensional coordinates $U_f/s_L(\rho_f/\rho_o)^{1.5}$ versus Hs_L/ν suggested by Kalghatgi (1984). Typical fuel jet based Reynolds number range of the reported data varies up to 2×10^5 and this covers a wide range of fuel jet velocities, jet diameters and different fuels. Although most of the data collapses into a narrow band irrespective of fuel velocity and fuel type as well as fuel dilution, the proposed non-dimensional coordinates are unable to explain the effect of fuel jet diameter on flame liftoff height. Flame liftoff height data from different fuel jet diameters does not

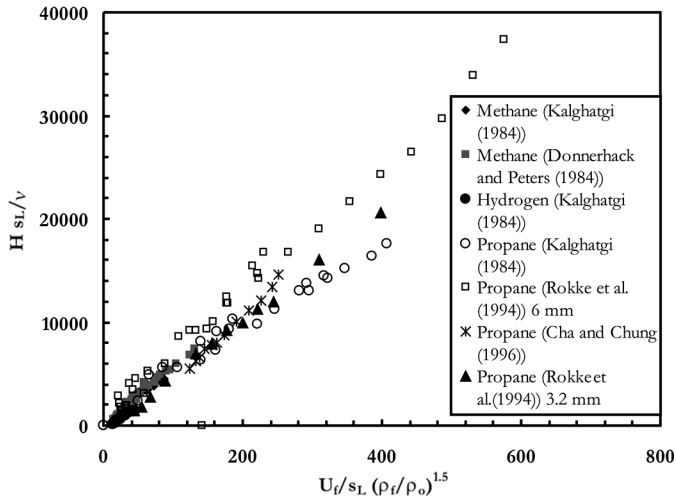

Figure 2. Experimentally measured flame liftoff heights for propane, methane and hydrogen fuels over a wide range of fuel jet diameters and velocities.

fall on a single line as shown in Figure 2 for 3.2 mm and 6 mm jet diameter propane flames.

Many attempts have been made by various researchers, for instance, Muller et al. (1994) and Montgomery et al. (1998) to predict the liftoff height variation with velocity for methane flames. The comparison of the flame liftoff height predictions shows good agreement with the experimental results. However, no detailed comparison for different fuels, coflow temperatures and fuel and coflow oxidizer mass fraction conditions has been reported in the literature. Muller et al. (1994) have used a combined premixed flame propagation and diffusion flamelet quenching model to predict flame liftoff and explain flame stabilization phenomena. The predicted liftoff heights agree well with the experimental results on methane by Kalghatgi (1984), Donerhack and Peters (1984) and Miake-Lye and Hammer (1988). No comparisons with the experimental results for other fuels such as propane and hydrogen have been made.

The authors (Muller et al., 1994) have pursued constructing a model for liftoff using thin flame assumption. The analysis invokes the conserved property variable for the diffusion mode and the level set variable approach for premixed flame. While the theory seems elegant, it is very complex. It appears that by invoking simplified global rate chemistry, it is possible to combine both the limiting conditions and the treatment of the problem becomes simple. This is the approach taken in the present study where a new flame extinction model is proposed to predict flame liftoff heights over a wide range of fuels, Reynolds number, jet diameter and velocity.

THE COMPUTATIONAL GEOMETRY

In this article, lifted turbulent jet flames are studied with different fuel jet diameters and different fuels. A general purpose CFD code, CFX-5.6 is used for this purpose (CFX-5.6, 2003). Three dimensional Navier-Stokes equations are discretised in the finite volume domain and solved in the physical space. Standard $k - \varepsilon$ model is used to model turbulent behavior of the jet flows. Energy and species conservation equations related to the particular fuel are solved in the computational domain. Mean reaction rate is modeled using the eddy dissipation concept (EDC) model with multi-step skeletal kinetics (Byggstoyl and Magnussen, 1985).

The transient term in the governing equations is discretised using first order backward Euler approximation (lumped mass approximation). This term affects the approach to the steady state solution but not the accuracy of the solution. A second order accurate scheme is used for spatial discretisation with physical advection terms. A time step of 1×10^{-5} s is employed for methane, propane and hydrogen flames. An iterative

technique is used to solve the discretised equations. The solution is considered to be converged when RMS residuals of flow, temperature and species have dropped by four orders of magnitude and there is no appreciable change in the respective residuals. The computations are carried out on an 8-node, 2.4 GHz Pentium IV parallel Linux cluster. The typical time required for a completely converged solution is approximately 8 hours ($\sim$50 hours of CPU time).

Computational Geometry

The physical and computational domains used for 6 mm jet diameter propane jet flame simulations are shown in Figure 3. A dense grid is carefully assigned in and around the central fuel jet where large gradients are

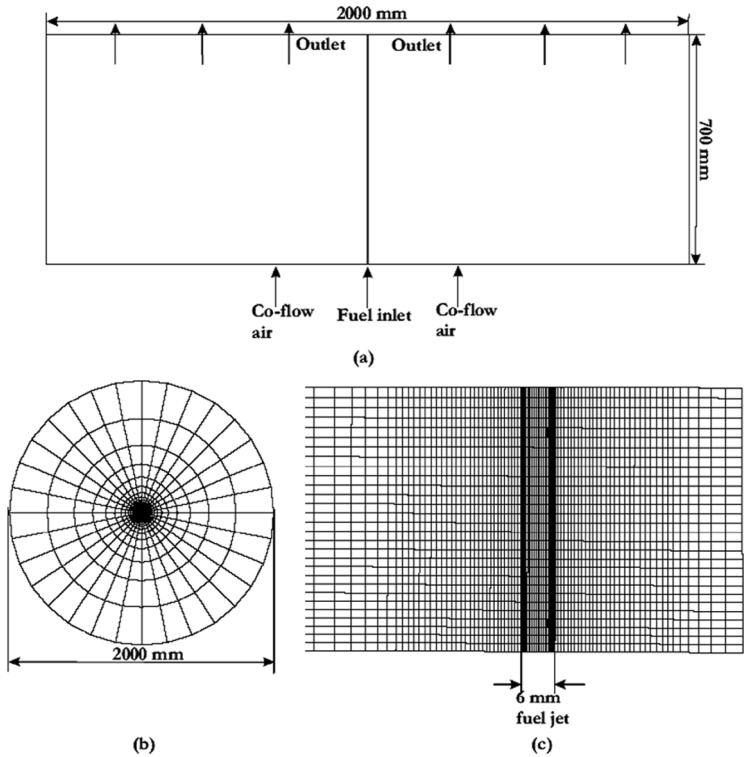

Figure 3. Details of computational domain and grid used for jet diffusion flames (a) Computational domain—Physical dimensions of the computational domain along with different boundary conditions are also shown. (b) Top view of the grid used for computations. (c) A close view of grid near fuel jet inlet.

expected. The outer dimensions considered in the present computational domain are large enough to avoid confinement effects and local recirculation in the domain due to wall boundary condition at the outer boundary. Similarly appropriate computational domains are selected for the prediction of flame liftoff height with fuel nozzles of different diameters.

Different grid properties like grid skewness and aspect ratios are checked and it is ensured that total number of skewed flux elements (skew $< 20^{\circ}$ and flux elements with large aspect ratios (greater than 75) are extremely small (less than 0.5%). Grid independence studies are carried out with 0.5, 0.6 and 0.7 million grid points to ensure grid independent results.

Boundary Conditions

The details of the computational domain are shown in Figure 3. Uniform velocity conditions are applied for both fuel and coflow boundaries. A uniform velocity boundary condition of 0.1 m/s is applied for the coflow air to allow steady inflow of air into computational domain for the lifted flames at ambient conditions. For highly preheated coflow conditions, the coflow velocity is calculated from the reported coflow mass flow rates and corresponding uniform velocity profile is applied. Fuel jet velocity condition is varied depending upon the experimentally reported values. A pressure based mixed type opening boundary condition is defined at the outlet. The fluid is assumed to be air at 300 K static temperature and pressure of 101325 Pa while products are exited at 101325 Pa pressure. Appropriate temperature and species mass fractions are also specified at the respective boundaries. A non-slip and adiabatic wall boundary condition is defined at the outer part of the domain.

THE EXTINCTION MODEL

In this article, a new extinction model is proposed based on the local turbulence time scale, $\tau_f = k/\varepsilon$. It is proposed that local flame extinction occurs in the computational domain when this turbulence time scale or fluid time scale, τ_f based on local fluid flow is smaller than the chemical time scale, τ_{ch} (or in other words, $Da < 1$, where $Da = \tau_f/\tau_{ch}$). The chemical time scale is derived as a function of the fuel and coflow properties like fuel mass fraction, fuel jet velocity, coflow temperature and oxidizer mass fraction. The computed chemical time scale is compared with the fluid time scale $\tau_f = k/\varepsilon$ at each grid point. And the averaged reaction rate term $\bar{\dot{\omega}}'''$ is set to zero if $\tau_f/\tau_{ch} < 1$ (local turbulence time scale is smaller than the chemical time scale). For a case of $\tau_f/\tau_{ch} > 1$,

the average reaction rate is calculated by using the EDC model, which is a finite value and depends upon the fuel and oxidizer mass fractions. This extinction model allows the prediction of the local extinction in the computational domain. The fluid time scale is defined by

$$\tau_f = \frac{k}{\varepsilon} \tag{1}$$

Here, k is turbulent kinetic energy and ε is the dissipation rate of turbulent kinetic energy.

A lifted flame is stabilized at a location where the local fluid flow velocity is equal to the local flame propagation speed. Laminar flame propagation speed of a fuel-air mixture depends on thermal properties of the mixture and reaction rate as shown below (Williams, 1985).

$$s_L \approx \frac{1}{\rho_o}\sqrt{\frac{\lambda}{C_p}\dot{\omega}'''} \tag{2}$$

where, λ is the thermal conductivity, C_p specific heat and $\dot{\omega}'''$, the global reaction rate of the fuel-air mixture which is defines as follows

$$\dot{\omega}''' \approx B Y_{O_2}^m Y_f^n T^\beta e^{(-E_a/RT)} \tag{3}$$

where, B is frequency factor, Y_i species mass fraction, T temperature, β temperature exponent and E_a activation energy. The values of m and n for different hydrocarbons are reported in Westbrook and Dryer (1984) for global reaction rates. There values are in the range of 1.5–2 and -0.5 to 0.5 for Y_{O2} and Y_f respectively. Chemical time scale depends on the reaction rate and inversely proportional to reaction rate $\tau_{ch} \sim 1/\dot{\omega}'''$.

A change in the coflow temperature affects the reaction rate and hence the flame liftoff height. To include the effects of coflow temperature on flame liftoff height, following relationship is suggested. A temperature term ΔT is suggested to be added into the adiabatic flame temperature of a standard air-fuel mixture combination (for example, propane-air at 300 K, $T_{ad} = 2254$ K). This temperature term, ΔT is added with respect to a reference temperature ($T_{ref} = 300$ K for the present computations) and a new coflow temperature T_{new}. An exponential term is added to include the relative effect of Arrhenius reaction rate term.

$$\Delta T = A(T_{new} - T_{ref})\frac{e^{(-E_a/RT_{new})}}{e^{(-E_a/RT_{ref})}} \tag{4}$$

where, A is a constant. Equation 4 can be further rearranged as

$$\Delta T = A(T_{new} - T_{ref})e^{((T_{ref}-T_{new})/T_{new})} \tag{5}$$

The remaining factor $e^{(-E_a/RT_{ref})}$ of the Arrhenius term in equation is included into constant A.

$$T_{ad,new} = T_{ad} + \Delta T \tag{6}$$

The chemical time scale at a new condition, T_{new}, Y_{O2} and Y_f is proposed to be estimated as follows.

$$\tau_{new} = \tau_{ref} (Y_{O_2})^{a_1} (Y_f)^{a_2} \left[\frac{e^{(-E_a/RT_{ad})}}{e^{(-E_a/RT_{ad,new})}} \right] \tag{7}$$

In Eq. (7), τ_{ref} is the chemical time scale at reference conditions (at $T = 300$ K for standard fuel-air mixture combination). Exponents, a_1 and a_2 are introduced to include the effect of change in oxidizer and fuel mass fractions in the coflow air and fuel jet. The exponential term represents the effect of change in coflow temperature.

Chemical time scale τ_{new} for present coflow conditions is approximated using the following procedure. The values of parameters A and τ_{ref} are determined from computational studies, aimed at predicting the flame liftoff heights correctly at reference conditions of 300 K for different jet flames such as methane, propane and hydrogen. Activation temperature parameter E_a/R (K) is taken as 20000 for propane and methane and 8000 for hydrogen from Plessing et al. (1998b) and Chakraborthy (1998) respectively. The values of these parameters for various fuels are summarized in Table 1 and they can be used to determine the chemical time scale for different conditions.

Six computational experiments, each at two extreme limits of (i) O_2 content, Y_{O2} and (ii) fuel mass fraction Y_f are carried out to determine the approximate effect of these mass fractions on a_1, and a_2. These values are found to be -2.0, and -0.5, respectively. When compared with Eq. (3), it can be deduced that $\dot{\omega}''' \sim Y_{O_2}^2 Y_f^{0.5}$, where $\tau_{chem} \sim 1/\dot{\omega}'''$. In summary, the constants that affect the predictions are A, Ea/R, and the

Table 1. Summary of different parameters used to determine the chemical time scale for different fuels at a reference velocity of 40 m/s

Parameters	C_3H_8	CH_4	H_2
A	2.2	2.2	25
T_{ref} (K)	300	300	300
E/R (K)	20000	20000	8000
τ_{ref} (ms)	0.04091	0.06546	0.000124

A – constant used for temperature correction in Eq. (7). T_{ref} – reference temperature for calculation of chemical time scale. E/R – activation temperature. τ_{ref} – reference chemical time scale.

exponents a_1, and a_2. The first two constants are sensitive to the choice of the fuel such as methane, propane and hydrogen and the two others seem not to change over several fuels considered for present investigations.

COMPUTATIONAL RESULTS AND EXPERIMENTAL COMPARISON

Computations are carried out over a range of coflow air temperatures, oxidizer mass fractions and diluted fuel flow conditions for propane, methane and hydrogen fuels. All results are compared with the experimentally measured flame liftoff heights as reported below.

Lifted Propane Jet Flames at Ambient Temperature and Pressure

The computations are carried out for the flame liftoff height measurements of Kalghatgi (1994) and Rokke et al. (1994) on 6 mm and 3.2 mm propane fuel jets. The contours of stoichiometric fuel mass fraction and k/ε based fluid time scale of 2, 3 and 4 ms are plotted as shown in Figure 4 for the case of propane fuel at a jet Reynolds number of 15,500. For the case of highly preheated and low O_2 mass fraction coflow,

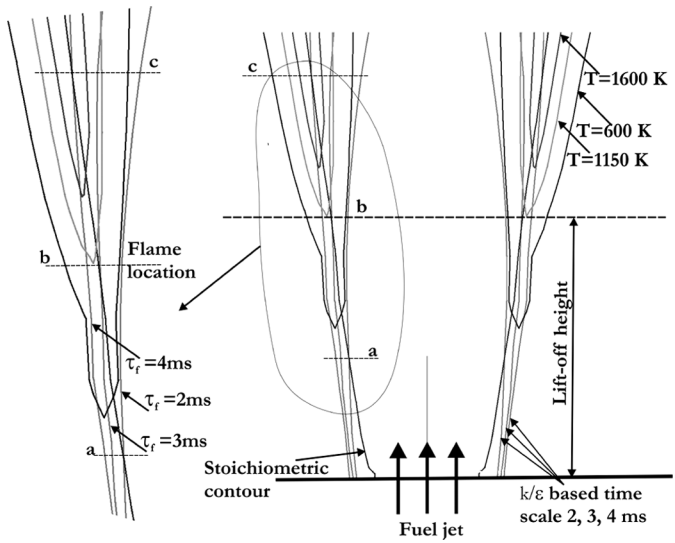

Figure 4. Computed temperature contours with $[k/\varepsilon]$ based extinction model. Present computations are carried out for 6 mm fuel jet diameter with propane fuel and 10 m/s fuel jet velocity. Lines a, b and c are drawn to indicate the intersection points of the τ_f contours with the stoichiometric mixture fraction contour.

it has been observed that the overall temperature rise across the reaction zone is about 200–300 K (Lille et al., 2000). It is very difficult to identify the exact flame location in the combustion zone. Therefore, to maintain uniformity in the paper, it is assumed that the flame is located at a point where the temperature is approximately equal to half of the maximum temperature rise in the domain.

$$T = T_{co-flow} + \frac{T_{\max} - T_{co-flow}}{2} \tag{8}$$

For illustrative purposes, in the case of propane jet flame at ambient conditions, the flame is assumed to stabilize at a location where the temperature is equal to 1150 K in the reaction zone as shown in Figure 4 for a case with Reynolds number of 15,500. The variation in flame liftoff height with this criterion is almost insignificant. An overall change of about 2 mm is observed with 1150 ± 50 K as a criterion for flame location. The stoichiometric mixture fraction contour and fluid time scale contours (2 ms, 3 ms and 4 ms and $U_j = 10$ m/s) are plotted in Figure 4. Since $\tau_{chem} = 3$ ms is used as an extinction criterion, the flame is assumed to be located approximately at a point, where the fluid time scale contour (3 ms for $U_j = 10$ m/s) intersects with the stoichiometric mixture fraction contour. Figure 4 also shows that flame extinction occurs in the computational domain as long as the k/ε based local fluid time scale is less than 3 ms. Similarly, a chemical time scale of 2 ms and 4 ms will result in a flame liftoff height corresponding to points a and c respectively, as shown in Figure 4. This shows that the present model based on this criterion (flame extinction for $Da = \tau_f/\tau_{chem} < 1$) is extremely sensitive in predicting the flame liftoff height.

The local fluid flow velocity across stoichiometric mixture fraction contour U_{st} is 1.3 m/s and velocity fluctuations derived from turbulent kinetic energy ($u' = (2k/3)^{1/2}$ are approximately 1.2 m/s at the flame stabilization point. Using the relation $s_T/s_L = [1 + C(u'/s_L)^n]$ from Williams (1985) with $s_L = 0.42$ m/s, $C = 1$ and $n = 0.7$, the turbulent premixed flame propagation speed turns out to be approximately 1.29 m/s. Therefore, the present analysis shows that a lifted jet diffusion flame is stabilized at a location on the stoichiometric mixture fraction contour where the turbulent premixed flame propagation speed, s_T is approximately equal to the local fluid flow velocity, U_{sp}.

Figures 5 and 6 show the experimentally measured flame liftoff heights by Kalghatgi, (1984) and Rokke et al., (1994) for different fuel jet diameters and propane fuel. Figure 5 shows that differences of about 15–20% exist between the measurements of Kalghatgi (1984) and Rokke et al. (1994). Similar differences can also be seen in Figure 6 which shows that the measured flame liftoff heights for 3.2 mm (Rokke et al., 1994) and 4.06 mm (Kalghatgi, 1984) jets are almost same. These discrepancies

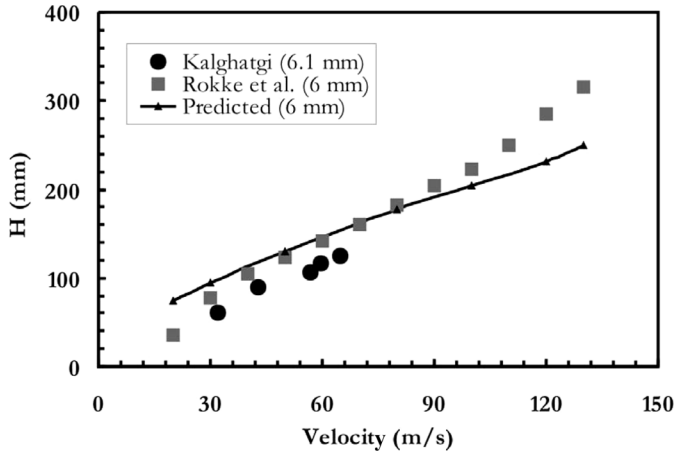

Figure 5. Prediction of flame liftoff heights compared with the experimental measurements of Rokke et al. (1994) and Kalghatgi (1984) for 6 mm fuel jet diameter with a constant time scale of 8.5 ms as extinction criteria, to describe the effect of constant chemical time scale based criteria on flame liftoff height variation with fuel jet velocity.

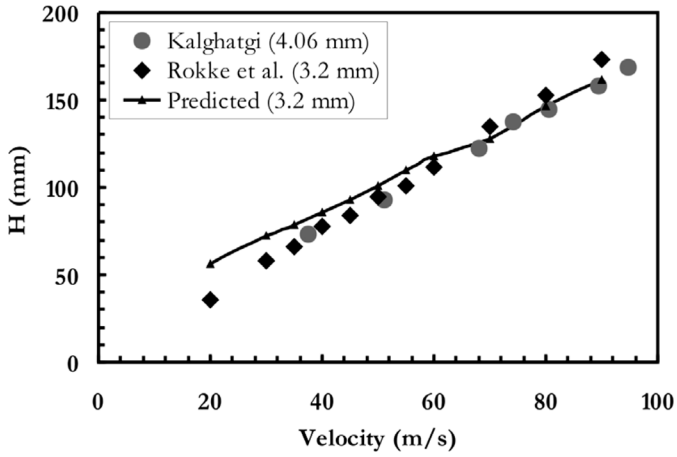

Figure 6. Prediction of flame liftoff heights compared with experimental measurements of Rokke et al. (1994) and Kalghatgi (1984) for 3.2 mm fuel jet diameter with propane as fuel. (The number in parenthesis shows the nozzle diameter used for experimental and computational results with a constant chemical time scale of 8.5 ms).

are also observed when flame liftoff height data from various sources is compared (Kalghatgi, 1984; Rokke et al., 1994; Cha and Chung, 1996). Various researchers use different criteria to determine the flame location depending on their convenience, such as thermal boundary, variation of particle seed density and CH-profile. The adoption of a particular criterion by individual researchers for determining the flame location probably leads to these discrepancies in the flame liftoff height data.

Therefore, the present computations are carried out to predict the flame liftoff heights and compare the predictions with a select set of experimental results taken from different sources (Donnerhack and Peters, 1984; Kalghatgi, 1984; Rokke et al., 1994; Lille et al., 2000; Cabra et al., 2002) expecting the comparisons to be within the $\pm 5\%$ of the experimentally reported flame liftoff heights. Figures 5 and 6 show the flame liftoff height predictions carried out with a constant time scale of 8.5 ms. Flame liftoff heights are overpredicted at low velocities and under-predicted at high velocities–near the blow-off limit. Flame liftoff predictions are independent to the fuel jet diameter compared to the predictions of Byggstoyl and Magnussen (1985) which are based on a fine structure time scale $C(\nu/\varepsilon)^{1/2}$. It is clear from Figures 5 and 6 that k/ε based fluid time scale and flame liftoff height do not increase at the same rate for turbulent jet flames.

The overprediction at low velocities and under prediction at high velocities is due to the fact that Eq. (7) does not include the effects of turbulence parameters on chemical time scale. The chemical time scale for a laminar propagating flame is given as

$$\tau_{chem} = \frac{D}{s_L^2} \tag{9}$$

where D is diffusivity of the mixture.

Similar to this relation, Damkohlar proposes a relation for turbulent flames (Peters, 2000)

$$\tau_{chem} = \frac{D_t}{s_T^2} \tag{10}$$

where D_t is the turbulent diffusivity of the mixture.

Many relations have been proposed to determine the turbulent flame propagation speed s_T. Recently, Filatyev et al. (2005) have reported the experimental measurements of the turbulent flame propagation speeds in a premixed slot burner. These measurements show that turbulent flame propagation velocity depends on following factors.

$$\frac{s_T}{s_L} = f\left(\frac{u'}{s_L}, \frac{l}{\delta_L}, Ma, \frac{\overline{U}}{s_L}, \frac{W}{\delta_L}\right) \tag{11}$$

where Ma is the Markstein number for given fuel type and equivalence ratio. δ_L is the flame thickness and W jet diameter. It is clear from Eqs. (10) and (11) that to determine the chemical time scale for turbulent jet flames, the effect of mean flow velocity $\overline{U}$, turbulence velocity fluctuations u' and integral length scale l should be included. The turbulent velocity fluctuations u' and integral length scale l depend upon mean flow velocity $\overline{U}$ and fuel jet diameter d respectively. The flame liftoff height predictions with Eq. (7) are independent of the jet diameter as shown in Figures 5 and 6. Therefore, the following relationship is suggested to include the overall effect of turbulent velocity fluctuations and mean jet velocity into Eq. (7).

$$\tau_{chem} = \tau_{ref}(Y_{O_2})^{a_1}(Y_f)^{a_2}(\overline{U})^{a_3}\left[\frac{e^{(-E_a/RT_{ad})}}{e^{(-E_a/RT_{ad,new})}}\right] \tag{12}$$

The exponent a_3 is determined from two calculations at $\overline{U}_{max}$ and $\overline{U}_{min}$ with an aim to correctly predict the dependence of flame liftoff height on the fuel jet velocity. It has been observed from these computations that a value of $a_3 = 0.6$ predicts the flame liftoff heights accurately, when these predictions are compared to the experimental results. The predicted results presented in Figure 7 show that the proposed flame extinction model based on k/ε is independent of fuel jet diameter and the flame liftoff height predictions are in good agreement with the experimental measurements of Rokke et al. (1994) for both 6 mm and 3.2 mm fuel jet diameters.

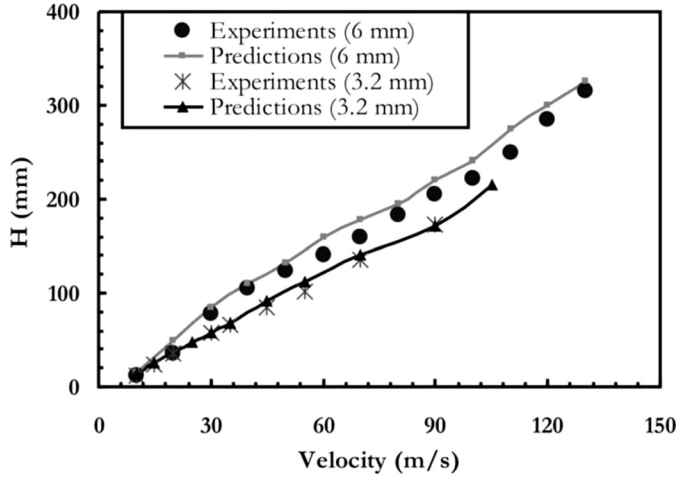

Figure 7. Flame liftoff height predictions compared with experimental measurements with the present flame extinction model for 6 mm and 3.2 mm fuel jet diameter fuel nozzles with propane fuels (Rokke et al. (1994)).

Methane Jet Flames

To predict the liftoff height of methane jet flames, the chemical time scale is determined using Eq. (12) and the predictions are carried out. The multi-step skeletal kinetics with EDC model is used to simulate methane combustion. Figure 8 shows the predicted flame liftoff height against the measured liftoff height of Donnerhack and Peters (1984) for the case of 6 mm fuel nozzle diameter. The predicted flame liftoff heights agree well with the experimentally measured flame liftoff heights.

Velocity and temperature fields are extracted from the numerical solutions of jet flames to verify the edge flame extinction concept proposed by Upatneiks et al. (2004) for $Re < 8500$. To compare the present computational results, velocity contours are plotted across 600 K isotherm (since Upatneiks et al. (2004) assume the flame location at 600 K isotherm). Figure 9(a) shows the temperature and velocity contours for methane jet flame with 16.7 m/s, 6 mm jet diameter and $Re = 5400$. It is observed that the flow velocity at the flame base is about 0.4 m/s, approximately equal to laminar flame propagation speed, as shown in Figure 9a. For the case of high Reynolds number, $Re \approx 19000$, shown in Figure 9b, the flow velocity is about 0.53 m/s, 1.4 times higher than laminar flame propagation speed. For a case of $Re \approx 30400$, the local flow velocity at flame stabilization point is about 0.82 m/s, 2.16 times laminar flame propagation speed (methane flame with 93.6 m/s fuel jet velocity and 6 mm jet diameter). This is also in agreement with the

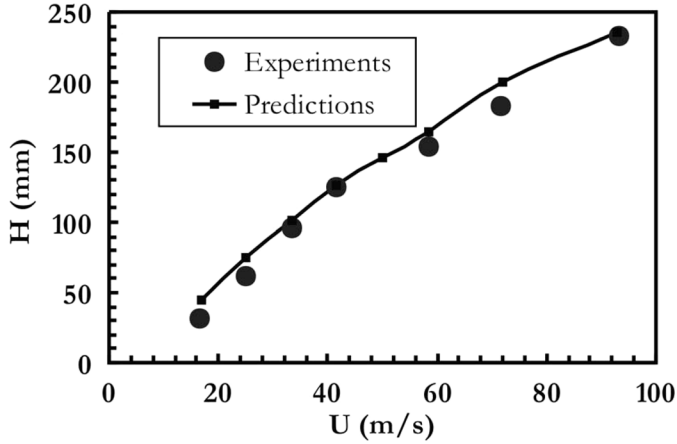

Figure 8. Predicted and experimentally measure flame liftoff heights for methane fuel with 6 mm fuel jet diameter. Experimental results are taken from Donnerhack and Peters (1984).

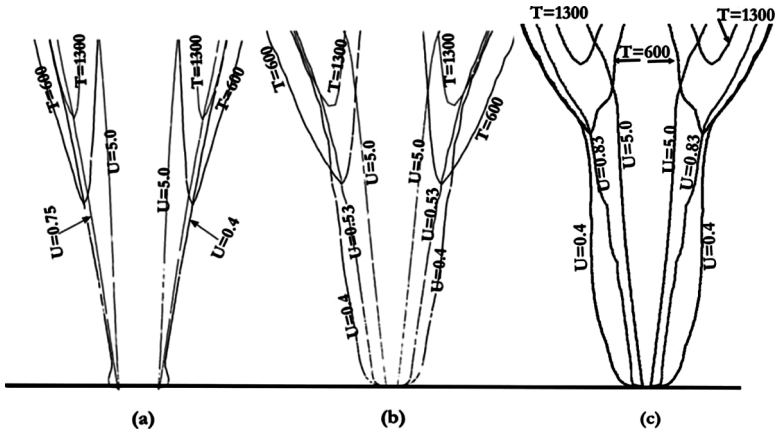

Figure 9. Temperature and velocity contours for 6 mm jet diameter methane flames. (a) $U_f = 16.7\,m/s$ (b) $U_f = 58.3\,m/s$ and (c) $U_f = 93.6\,m/s$.

measurements of Muniz and Mungal (1997) which reports that the local flow velocity at the stabilization point is less that $3s_L$ for present calculations. Further, turbulent flame propagation speeds are computed at the flame stabilization point using the relationship suggested in Eq. (7) of Filatyev et al. (2005). The complete form of this equation is presented here.

$$\frac{s_T}{s_L} = 1 + B_1\left[\left(\frac{u'}{s_L}\right) - B_2\left(\frac{u'}{s_L}\right)\right]^{1/2} \times \left[\frac{\overline{U}}{s_L}\right]\left[\frac{l}{\delta_L}\right]^{1/2}\left[\frac{D}{\delta_L}\right]^{1/2} \tag{13}$$

where $\overline{U}$ is the mean jet velocity, D fuel jet diameter and flame thickness, $\delta_L = 0.35\,mm$. To calculate turbulent flame propagation speed, different variables, u', l, U_{sp} are obtained at the flame stabilization point (at $T = 600\,K$ isotherm). The values of coefficients B_1 and B_2 are chosen as 0.07 and 0.16 to compare the calculated s_T with the observed velocities. The results are compared for both methane and propane flames over a range of velocities as shown in Table 2. It is seen that the predicted flame propagation speeds are within $\pm 5\%$ of the local flow velocity at the flame stabilization point. Although these velocities are slightly less than 1 m/s, much higher flow velocities ($\sim$1–1.2 m/s) are experimentally measured by Muniz and Mungal (1997) and Watson et al. (2000) upstream of the flame stabilization point. The existence of higher flow velocities ($\sim$1.0 m/s) at the flame stabilization point shows that that flame stabilization is governed by turbulent flame propagation rather than laminar flame propagation.

The above investigation on methane flames shows that Reynolds number has a strong effect on the local flow velocity at the flame

Table 2. Summary of different values obtained from computations and predicted turbulent flame propagation speed at flame stabilization point

	U_{jet} (m/s)	U_{sp} (m/s)	u'(m/s)	l (m)	s_T/s_L	s_T(m/s)
Methane flames	16.67	0.4	0.41	0.00145	1.14	0.43
	58.33	0.53	0.50	0.0078	1.47	0.55
	93.33	0.82	.083	0.0144	2.15	0.82
Propane flames	10	0.35	0.27	0.0006	1.05	0.46
	70	0.727	0.84	0.00745	1.61	0.71
	110	0.985	1.29	0.012	2.14	0.95

The values of various constants used in Eq. (7) of Filatyev et al. (2005) are $B_1 = 0.07$, $B_2 = 0.16$, $\delta_f = 0.35$ mm (laminar flame thickness), $d = 6$ mm (jet diameter).

stabilization point as shown by Schefer and Goix (1998) through PIV measurements. The change in local flow velocity at flame stabilization point with Reynolds number also hints at the dominant role played by different flame stabilization mechanisms at high Reynolds numbers as suggested by Chen and Bilger (2000) and shown in Figure 1.

Coflow velocity significantly influences the flame liftoff of the lifted jet flames. Muniz and Mungal (1997) and Brown et al. (1999) have experimentally investigated the effects of coflow velocity for methane jet flames. Montgomery et al. (1998) have numerically investigated the effects of coflow velocity on flame liftoff and they show that when the flame liftoff height data is plotted with an effective jet velocity, the whole data falls into a single line. The effective jet velocity is defined as the fuel jet velocity plus a component of the coflow velocity as shown here,

$$U_{eff} = U_f + C\sqrt{\frac{\rho_{coflow}}{\rho_{fuel}}}U_{coflow} \tag{14}$$

where ρ_{coflow}, ρ_{fuel}, U_{coflow} and U_f are densities and velocities of the coflow and fuel jet streams respectively. The liftoff height data from Muniz and Mungal (1997) and Brown et al. (1999) collapses to a single curve when fuel jet and coflow velocities are expressed through an effective jet velocity derived from Eq. (14). Figure 10 shows the collapse of the data for methane fuel jet and the least scatter of the data occur for $C = 40$. Therefore, to apply the present model for predicting the flame liftoff heights with coflow velocity component, a chemical time scale corresponding to the effective jet velocity should be assigned as the extinction criterion. This will result in the accurate predictions of the liftoff height for various flames subjected to strong coflow conditions.

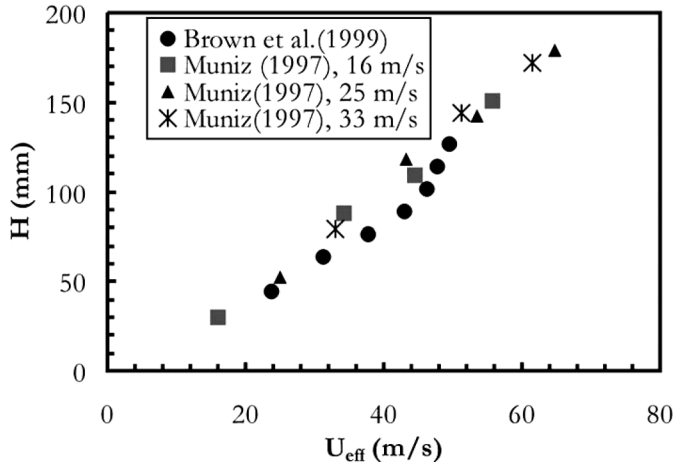

Figure 10. Flame lift-of height data plotted against an effective fuel jet velocity for various coflow velocities. Brown et al. (1999) is the data for 23.7 m/s fuel jet velocity and fuel jet velocities for Muniz and Mungal (1997) are mentioned in the figure.

Hydrogen Jet Flames

Hydrogen jet flames are simulated with a single step eddy dissipation model. A single step EDC based combustion model is used to simulate the combustion process. The chemical time scale is determined using Eq. (12) with the different parameters as shown in Table 1. The predictions for the measured liftoff heights by Kalghatgi (1984) are shown in Figure 11. The predicted liftoff heights agree well with the experimental measurements. Flame liftoff heights are slightly under-predicted for the case of 1.74 mm jet diameter.

Diluted Propane Flames

To determine the effect of fuel jet dilution on chemical time scale, numerical simulations are carried for diluted propane flames and presented in this subsection. A number of numerical experiments are carried out aimed at predicting the flame liftoff height of diluted propane flames to determine the flame liftoff height dependence of fuel mass fraction. The chemical time scale varies as $Y_f^{-0.5}$. A similar dependence of flame liftoff height on $Y_f^{-0.5}$ has also been suggested by Rokke et al. (1994) for diluted propane jet flames. Figure 12 shows the prediction of flame liftoff height for diluted propane jet flames. Propane is diluted with air

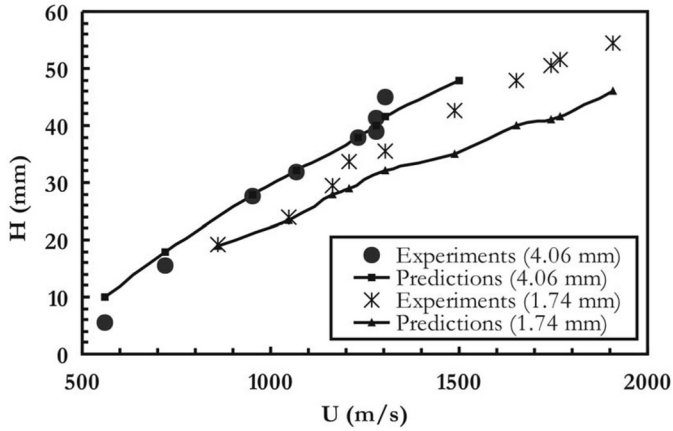

Figure 11. Comparison of predicted and experimentally measured hydrogen flame liftoff heights for 4.06 mm and 1.74 mm fuel jet diameter. The experimental data is taken from Kalghatgi (1984).

at 300 K and then injected through the fuel nozzle. Present calculations are carried out for 6 mm fuel jet diameter with 300 K as coflow temperature and 30 m/s fuel jet velocity. It has been found that the prediction of flame liftoff height is in excellent agreement with the experimentally measured values as shown in Figure 12.

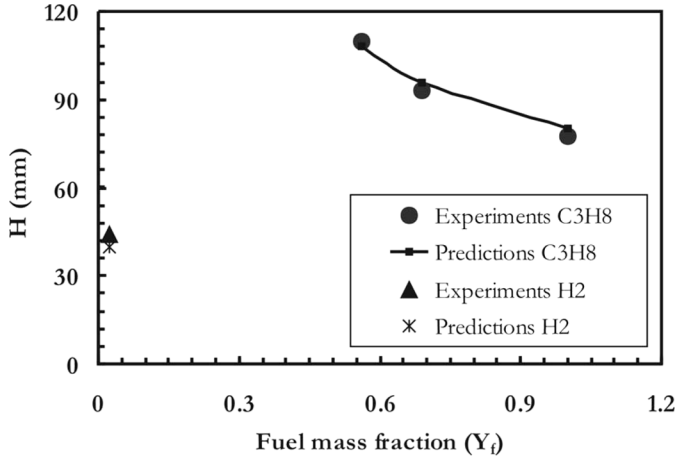

Figure 12. Variation of flame liftoff height for 6 mm propane diluted flames at 30 m/s velocity from Rokke et al. (1994) and diluted hydrogen flames by Cabra et al. (2002).

Diluted Hydrogen Flames at High Temperature and Low Oxidizer Concentration

The results reported by Cabra et al. (2002) on highly diluted hydrogen ($Y_f = 0.024$) jet flames with $Y_{O2} = 0.171$ and a coflow temperature of 1045 K are simulated using a single step EDC model. Figure 12 shows that the predicted liftoff height is 40 mm. This matches quite closely with the experimentally measured flame liftoff height ($\sim$44 mm). This result shows the robustness of the present model to predict flame liftoff height of diluted flames at ambient as well as high temperature coflow conditions.

LPG Flames at High Temperature and Low Oxidizer Concentration

In this section, the results of the predicted flame liftoff height for LPG under high temperature and highly vitiated coflow conditions are presented. The composition of LPG as reported by Lille et al. (2000) is 75% C_3H_8, 20% C_3H_6, 3% C_2H_6 and 2% C_4H_{10} by volume. These experiments are carried out by Lille et al. (2000) over a wide range of O_2 mass fraction in the coflow (0.055–0.233 and O_2 mole fraction 5–21%), coflow temperature (1063–1113 K) and fuel jet diameters. Fuel jet diameters are varied from 0.3 mm to 0.8 mm and Reynolds number varying up to $\sim$4200.

The numerical simulations are carried out for the fuel jet diameters of 0.4, 0.5 and 0.6 mm. Uniform velocity conditions are applied for both fuel and coflow air. A combined finite rate chemistry and eddy dissipation model along with skeletal propane-air kinetics is applied for modeling the LPG flames in high temperature and low O_2 concentration in the coflow. The chemical time scale is calculated using propane parameters shown in Table 1 and Eq. (12).

Figures 13 (a)–(d) shows the comparison between the predicted and experimentally measured liftoff heights of the jet flames under high temperature and vitiated conditions. The mass fraction of O_2 in coflow varies over a large range of 0.055–0.233 and the coflow temperature is maintained at 1113 K. It is clear from Figure 13a that the flame liftoff increases sharply with a decrease in O_2 mass fraction in the coflow. Figures 13b and 13c show the predicted flame liftoff heights for 0.5 mm and 0.6 mm fuel nozzles with fuel jet velocities of 26 m/s and 18 m/s, respectively. The predicted results compare well with the experimental results. A good agreement between the experimentally measured and predicted flame liftoff height confirms the independence the present model from diameter effect in comparison to the $C(\nu/\varepsilon)^{1/2}$ based time scale proposed by Byggstoyl and Magnussen (1985). All the values of the chemical time

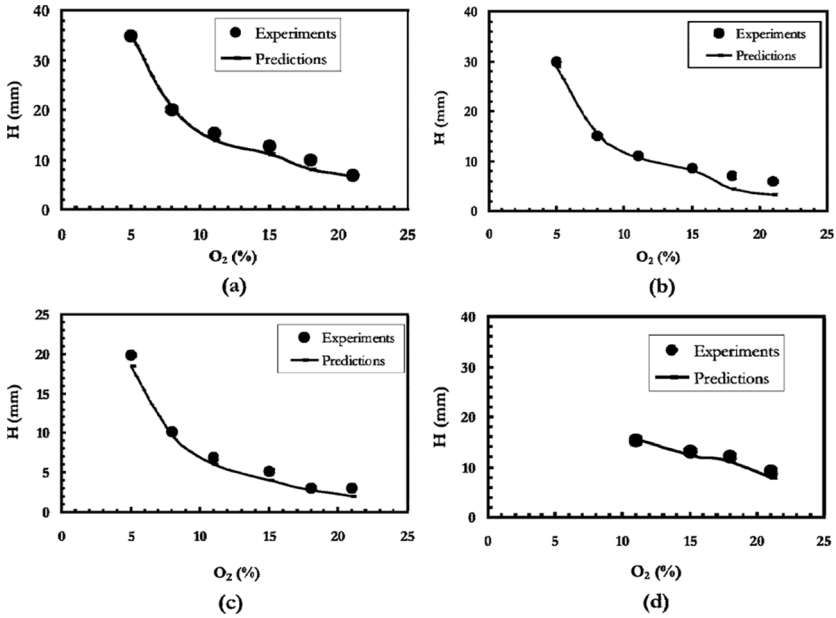

Figure 13. Predicted and experimentally measured flame liftoff heights of propane jet flames with varying O_2 mass fraction coflow conditions. (a) $T_{coflow} = 1113\,K$, $U_j = 40\,m/s$ and 0.4 mm fuel jet diameter. (b) $T_{coflow} = 1113\,K$, $U_j = 26\,m/s$ and 0.5 mm fuel jet diameter. (c) $T_{coflow} = 1113\,K$, $U_j = 18\,m/s$ and 0.6 mm fuel jet diameter. (d) $T_{coflow} = 1063\,K$, $U_j = 40\,m/s$ and 0.4 mm fuel jet diameter. Experimental results are taken from Lille et al. (2000).

scale used for the present computations are derived using the parameters listed in Table 1.

Figure 13d shows the predicted results for a coflow temperature of 1063 K. The mass fraction of O_2 is varied over a range of 0.122–0.233. The computations are carried out for the case of 0.4 mm fuel jet diameter and a jet velocity of 40 m/s. The predicted flame liftoff heights are in good agreement with the experimentally measured values.

In summary, the present model gives a good prediction of flame liftoff heights for different fuels, over a wide range of coflow temperature, fuel mass fraction and oxidizer mass fraction. Particularly, the comparison of LPG predictions at high temperature and highly diluted conditions with the experimental results is of considerable importance to flameless combustion burners. These conditions are very similar to the conditions that exist in mild/flameless combustion burners. Therefore, the present extinction model is used subsequently to predict the combustion and fluid flow behavior of 3 kW laboratory and 150 kW scaled burners.

MODELING OF THE 3 kW MILD COMBUSTION BURNER

There have been a few efforts by Wunning and Wunning (1997), Coelho and Peters (2001), Mancini et al. (2002), Cavaliere and de Joannon (2004), Christo and Dally (2005) and Maruta et al. (2000) to model flameless combustion. Wunning and Wunning (1997) have modeled a 160 kW furnace at 1473 K operating temperature. The $k-\varepsilon$ model with logarithmic wall function approach for turbulence, Arrhenius reaction rate approach for combustion and one step reaction for NO formation have been used. The predicted average temperature profiles compare qualitatively well with the measured temperatures in the furnace. Coelho and Peters (2001) have carried out numerical simulations of a flameless combustion burner operated at about 5.4 kW thermal input with a mild air preheat ($\sim$650 K). They have argued that the steady flamelet model is unable to correctly describe the NO formation as it is a chemically slow process and sensitive to the transient effects.

Mancini et al. (2002) have carried out numerical simulations on a 0.58 MW natural gas fired furnace operated under steady state conditions with preheated air at 1573 K temperature. Computations are carried out with EBU, EDC and mixture fraction based pdf combustion models. There are substantial differences between the predicted and measured CH_4 mass fraction, NO_x emissions and temperature across the fuel jet irrespective of the combustion model used. Authors have argued that these inconsistencies in predictions near the fuel jet zone arise due to non-steady behavior of fuel jet, as observed during the experimental investigations. A recent numerical modeling study by Christo and Dally (2005) on high temperature and highly diluted turbulent reacting jets shows that EDC model with skeletal and detailed chemistry performs better when compared to the conserved scalar models like PDF and flamelet models. Therefore in this study, EDC model with skeletal kinetics and present extinction model is used to predict the fluid flow and combustion behavior in the mild combustion burners.

It is inferred from the experimental observations (as discussed in Kumar et al., 2002, 2005; Kumar, 2004) that flame liftoff under high temperature and vitiated coflow conditions is an essential condition to achieve flameless combustion. Recently, Dally et al. (2004) have also reported the appearance of unstable jet flames for propane and ethylene fuels near the fuel jet exit. A visible flame with methane was noticed when fuel flow rates were reduced below a certain limit. This is attributed to the fact that larger residence times and lower scalar dissipation rates in the near injection zone leads to the appearance of unstable and lifted flames near the fuel jet exit. Dally et al. (2004) further believe that the instability reported by various authors (Wunning and Wunning, 1997; Plessing et al., 1998b;

Dally et al., 2004) is directly related to larger residence time and flame propagation velocity of the partially premixed mixture at high temperature and highly diluted conditions that exist in the furnace. Therefore, it is of significant importance for a combustion model to accurately predict the initial premixing of fuel jet with hot combustion products, flame liftoff and other related characteristics to achieve better understanding of the process. The flame liftoff predictions from the proposed flame extinction model agree well with the experimental data as reported in previous section over a wide range of coflow temperature and O_2 mass fraction conditions.

The flamelet combustion model used in the earlier computational studies (Kumar et al., 2002, 2005) (without any local extinction model) is unable to predict the flame liftoff, even though the aspects concerning concentration and temperature distribution have been reasonably well predicted. This, in part, is due to the relatively small contribution of the flame volume close to the fuel jet entry into the combustion chamber. In consideration of this part, it is essential for a combustion model to accurately predict the fuel jet behavior and flame liftoff characteristics at high temperature and low O_2 mass fraction conditions. High temperature and highly vitiated jet flames predicted with the present flame extinction model, reported in Figure 13 are similar to those that exist in a flameless combustion burner.

Temperature Fields

Figures 14a and 14b show the measured temperature fields and predictions with the EDC model along with the present extinction model for the laboratory scale burner investigated experimentally earlier. Predicted temperature profiles are compared with the experimentally measured values shown in Figures 14a and 14b. The predicted temperatures are approximately 200 K higher than the measured temperature in the combustion zone. The patterns of the temperature predicted with the EDC model are nearly similar to the experimentally measured temperature profiles. The EDC model is able to predict the initial premixing of combustion products with the high speed fuel jet. Another interesting feature of the present numerical simulations is the prediction of the presence of a high temperature zone (1400 K and 1600 K temperature contour in Figures 14a and 14b respectively) between the air and fuel jets 20 mm downstream of the injection plane.

Figure 15 shows the temperature contours at different thermal inputs for the laboratory scale burner investigated by the authors' earlier (Kumar et al., 2002). Figure 15a shows the temperature contours for 3 kW thermal input. The fuel injection velocity is $\sim$60 m/s. The

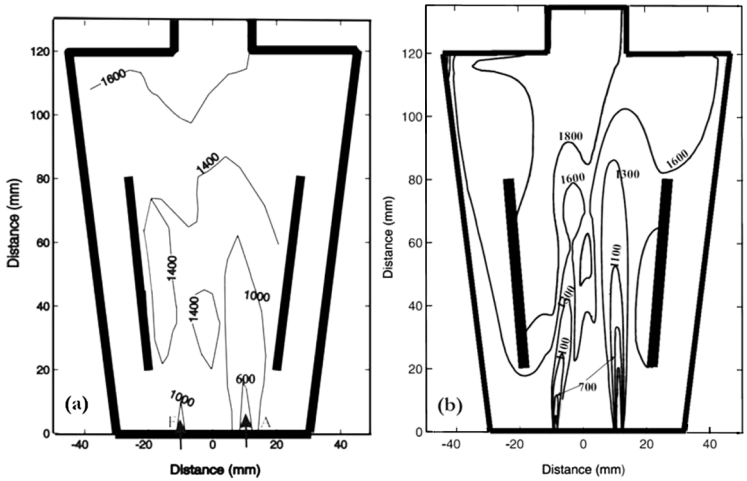

Figure 14. Measured (a) and Predicted (b) temperature profiles in 3 kW burner with the currently proposed extinction model and eddy dissipation combustion model.

temperature contours in the combustion zone show that flame is lifted from initial injection zone and located at about 25 mm from the injection plane at 3 kW thermal input. This is clear from the temperature plot, which shows a considerable temperature rise at a location 25 mm downstream from the injection point.

Figure 15b shows the temperature patterns for 1 kW thermal input in the same burner. The fuel is injected at about 20 m/s velocity into the combustion chamber. It is clear from the temperature contours that flame stabilization point moves upstream (recognized from a high temperature contour along the fuel jet). A substantial temperature rise is observed at about 5 mm from the jet injection point. This hints at an apparent transition from flameless combustion to conventional combustion mode, recognized by the appearance of highly confined, weak, and lifted jet flames in the combustion zone (flame liftoff height decreases with a reduction in fuel jet injection velocity). Figure 15c shows the temperature contours for 0.6 kW thermal input with $\sim$12 m/s fuel jet velocity. The temperature contour plot indicates that a further reduction in fuel jet velocity results in very small (or almost nil) liftoff height and reaction start immediately as soon the jet is injected into the combustion chamber. This experimentally observed feature of transition from flameless combustion to conventional combustion model has been discussed in one of the earlier publications (Kumar et al., 2005).

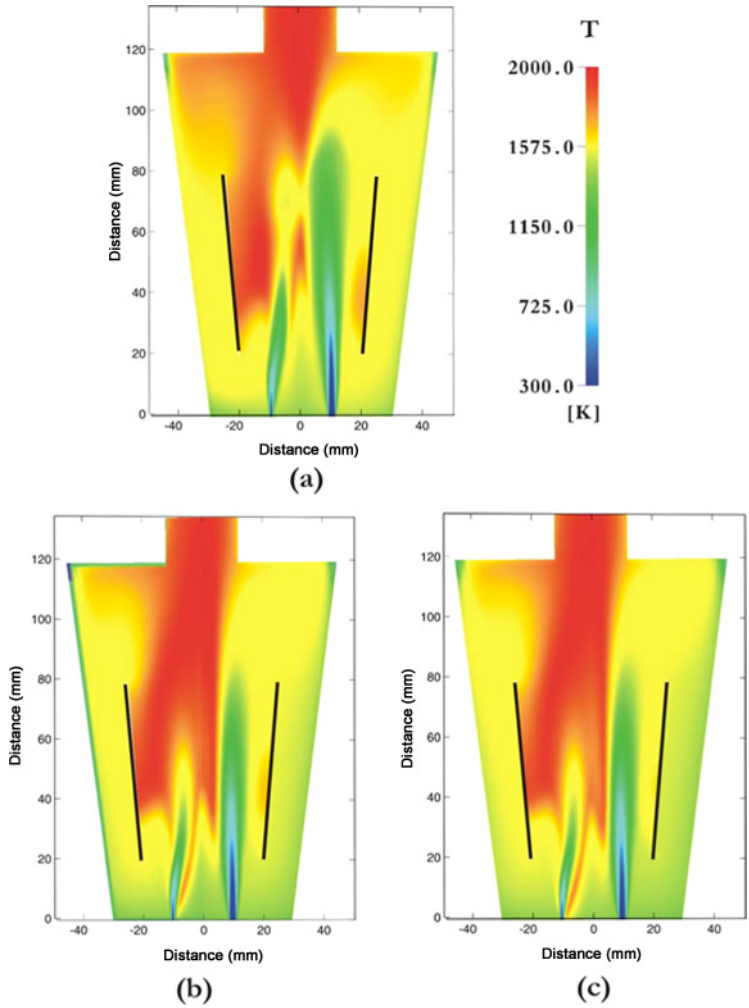

Figure 15. Predicted temperature fields for the laboratory scale burner at different thermal input levels. (a) at 3 kW normal operation (b) at 1 kW thermal input and (c) at 0.6 kW thermal input level.

Reaction Rate Fields

Reaction rate contours are plotted over a range of thermal inputs. Figure 16 shows propane oxidation reaction rate contour plots in the combustion zone. Figure 16a shows the propane oxidation reaction rate contours for 3 kW thermal input. It is seen that mixing of fuel and combustion products continues after the fuel injection due to large recirculation rates

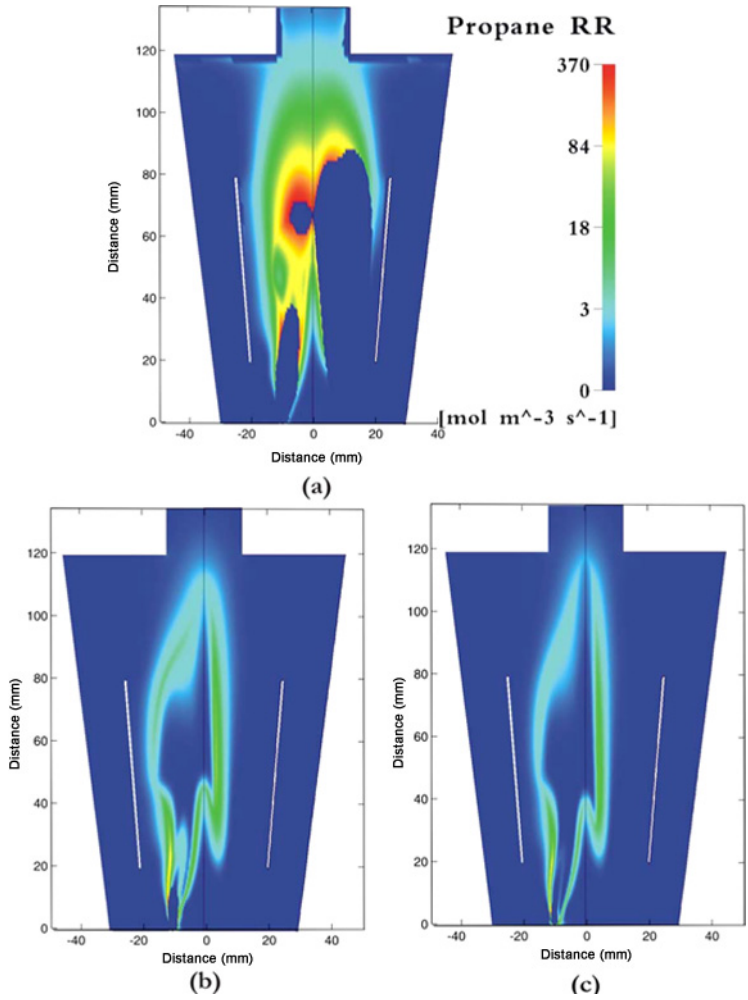

Figure 16. Predicted propane oxidation reaction rate contours in laboratory scale burner at different thermal input levels. (a) at 3 kW normal operation (b) at 1 kW thermal input and (c) at 0.6 kW thermal input.

of combustion products. Large velocity of fuel jet leads to the stabilization of the reaction zone downstream. A weak propane oxidation reaction starts at about 10 mm from the fuel injection point and continues further downstream. Reaction rate contours are plotted on a logarithmic scale to illustrate the fact that a weak combustion reaction continues over a large volume during the flameless combustion mode.

Figures 16b and 16c shows the propane oxidation reaction rate contours for 1 kW and 0.6 kW thermal input with approximately 20 m/s and 12 m/s fuel jet velocities respectively. These reaction rate contours show that the combustion reaction front moves upstream due to reduction in the fuel jet velocity. These figures also show that the peak reaction contours have moved more closer to the fuel injection point. The decrease in fuel jet velocity leads to a decrease in the volume over which combustion reaction occurs. This hints at more intense reaction within a small zone and hence a shift from flameless combustion mode towards the appearance of highly confined jet flames in the combustor.

The appearance of confined jet flames (transition from flameless combustion to conventional combustion mode) at lower thermal power level and larger convective time scales has been discussed by Kumar et al. (2005) and Kumar (2004) along with a brief summary of experimental conditions. Further evidence towards this is obtained from present computational studies on a 3 kW burner. It is shown in Figures 15 and 16 that with a reduction in thermal power input (hence reduction in both air and fuel injection velocities) in the burner, the reaction zone travels upstream. At 1 kW thermal input, the flame is lifted as clear from Figures 15b and 16b. At 0.6 kW thermal input, (corresponding convective time scales are $\tau_a = 125\,\mu s$ and $\tau_f = 42\,\mu s$) the flame is almost attached to the base of fuel jet as clear from the reaction rate contours shown in Figure 16c. This gives further evidence of global convective time scales playing decisive role in the flameless combustion burner operation as reported in Kumar et al. (2005).

A reduction in thermal input leads to a decrease in the fuel and air injection velocities which results in a decrease in the flame liftoff height and movement of reaction front towards the injection plane. This finally leads to the appearance of highly confined jet flames in the combustion zone. Dally et al. (2004) have reported a similar appearance of confined flames with a reduction in the fuel jet velocity for propane and methane. This has been attributed to small residence time and low scalar dissipation rates close to the fuel jet exit. The flame propagation towards the jet exit and appearance of the highly confined jet flames is directly related to flame residence time and flame propagation velocity of the local mixture. This is believed to be one of the possible reasons for transition from flameless combustion mode to conventional combustion.

MODELING OF 150 kW FLAMELESS COMBUSTION BURNER

The computational modeling of 150 kW burner is carried out with the EDC model with skeletal kinetics, which includes the presently proposed flame extinction model. More details about the computational domain

and boundary conditions employed for present computations are similar to those used in the earlier work on 150 kW burner (Kumar et al., 2005). Air and fuel injection velocities are about 100 and 250 m/s, respectively.

Temperature and mass fractions of the different species are extracted from computational results. These computational results are plotted against the experimental measurements at 150 mm and 400 mm downstream of the injection point. Figures 17a and 17b show the computational results as lines and the experimental data points for different species and temperature at 150 mm and 400 mm downstream. The experimentally measured species mole fractions are converted into mass fractions and

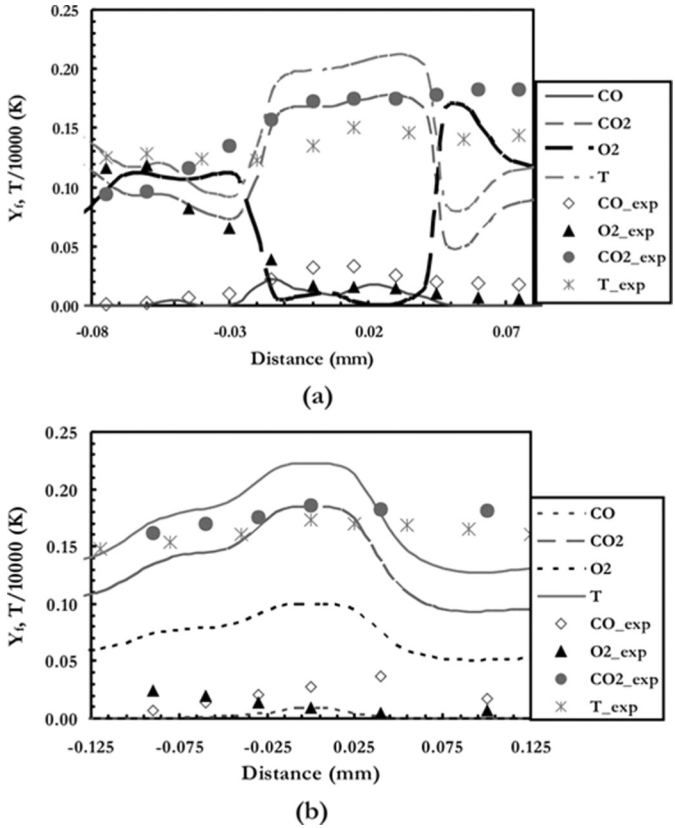

Figure 17. Comparison of the predicted results with the modified extinction model and experimental measurements for 150 kW burner operated with LPG fuel. (a) Predictions and experimental measurements of different species and temperature at 150 mm downstream from the injection point. (b) Predictions and experimental measurements of different species and temperature at 400 mm downstream from injection point.

the results are plotted in the same manner as reported in Figure 8 of earlier publication (Kumar et al., 2005). Measurements of CO and CO_2 mass fractions and temperature compare well with predictions at 150 mm downstream of the injection point. Similarly, the predicted O_2 mass fraction also compares well with measurements on the air jet side at 150 mm position. Certain differences between the measured and predicted O_2 mass fraction exist on the fuel jet side. Substantial differences are observed between measurements and predictions of O_2 mass fraction at 400 mm downstream location. However, the predictions of CO_2, CO and temperature are comparatively better and follow the general trend of the experimentally measured values.

The computed temperature and propane oxidation reaction rates inside the combustor for the 150 kW burner with propane fuel are presented in Figure 18. It is clear from the temperature contours that temperature increases significantly at about 50 mm downstream from the injection point due to commencement of the combustion reaction. Temperature contours show nearly uniform distribution of temperature in the combustion zone. The temperature in most part of the combustion zone is in the range of 1100–2000 K. Figure 18b shows the predicted propane oxidation reaction rate contours in the combustion zone on a logarithmic scale. Propane reaction contours show that mixing of the fuel jet with combustion products continues once the fuel is injected into the combustion zone. A weak reaction occurs downstream and continues over a large volume. Reaction rate contours indicate that

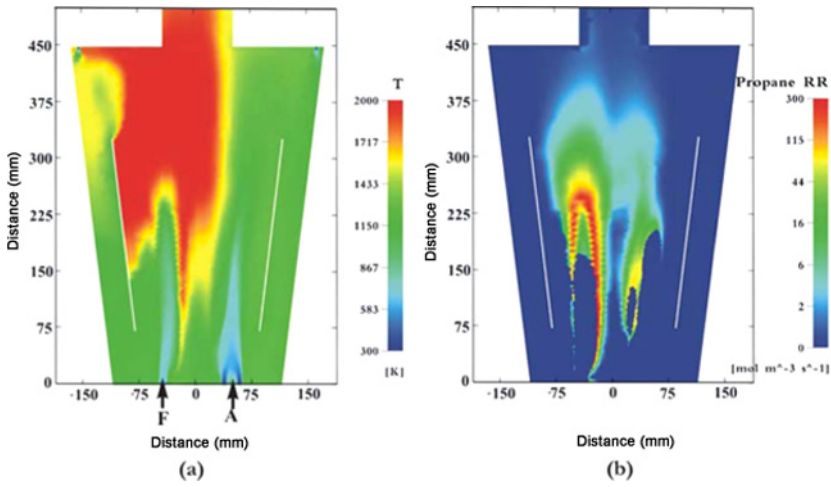

Figure 18. Contours of predicted (a) temperature and (b) propane oxidation reaction rates for 150 kW burner.

reaction starts very near to the injection plane. This is due to the fact that average O_2 mass fraction in the combustion zone is higher in the 150 kW burner in comparison to the 3 kW burner. This is clear from Figure 6 of Kumar et al. (2005) which shows the cumulative behavior of O_2 mass fraction for the 150 kW burner (curve b) and the 3 kW burner (curve c) respectively.

CONCLUSIONS

In this article, a new flame extinction model is proposed to predict the flame liftoff height under different coflow conditions. The flame is assumed to be quenched, when the fluid time scale is less than the chemical time scale ($Da = \tau_f/\tau_{ch} < 1$). The chemical time scale is determined from the coflow temperature, fuel mass fraction, O_2 mass fraction and fuel jet velocity.

The proposed extinction model is applied for a wide range of jet flames like propane, methane and hydrogen. The examined coflow conditions are varied from 300 K to 1113 K temperature and O_2 mass fraction ranging from 0.055–0.233. Present studies show that flame liftoff height is a strong function of O_2 and fuel mass fraction and coflow stream temperature. The predicted flame liftoff heights are found to be in good agreement with the experimental results for all the simulated conditions. It is observed that flame stabilization occurs at a point near the stoichiometric mixture fraction surface and where the local flow velocity is equal to the local flame propagation speed. Therefore, the limit of $Da \rightarrow 0$ seems to be an appropriate line of thought to explain the stabilization of lifted flames.

Based on the locally prevailing flow and thermal conditions, the present model is used to determine the chemical time scale for the present 3 kW and 150 kW flameless combustion burners. Numerical modeling of the flameless combustion burners is carried out with the proposed extinction model and EDC model with skeletal kinetics. The predictions of these studies compare well with the experimental results. The present flame extinction model with skeletal kinetics is able to predict the important features of flameless combustion burners; temperature profiles, reaction zone and initial premixing of fresh fuel and air with combustion products. The computational studies reveal that reduction in thermal input (hence reduction in fuel and air jet velocity) results in the appearance of the highly confined jet flames. Reaction rate contours show that during flameless combustion a weak reaction continues to take place over a large volume in comparison to the conventional combustion mode.

NOMENCLATURE

β	Temperature exponent
ν	Kinematic viscosity
ε	Dissipation rate of turbulent kinetic energy
τ_f, τ_{ch}, τ_{ref}, τ_{new}	Fluid, chemical, reference, new chemical time scale
ρ_f, ρ_o	Density of fuel jet, coflow air
$\dot{\omega}_i'''$	Chemical source termfor species i
B	Frequency factor
Da	Damköhlar number
E/R	Activation temperature
H	Flame liftoff height
k	Turbulent kinetic energy
l_f	Laminar flame thickness
l	Turbulence length scale
s_L	Laminar flame propagation speed
s_T	Turbulent flame propagation speed
T, T_{ref}, T_{new}, T_{ad}	Temperature, reference, new and adiabatic temperature
u'	Turbulent velocity fluctuations
U_{sp}	Flow velocity at flame stabilization point
U_{st}	Flow velocity across the stoichiometric contour
U_p	Local flame propagation speed
$\overline{U}$	Mean fuel jet velocity
Y_i	Mass fraction of Species i

REFERENCES

Buckmaster, J.D. (1996a) Edge flame and their stability. *Combust. Sci. Tech.*, **115**, 41.

Buckmaster, J.D. and Weber, R. (1996b) Edge-flame-holding. *Proc. Combust. Instit.*, **26**, 1143.

Brown, C.D., Watson, K.A., and Lyons, K.M. (1999) Studies on lifted jet flames in coflow: The stabilization mechanism in the near and far-fields. *Flow Turbul. Combus.*, **62**, 249.

Burgess, C.P. and Lawn, C.J. (1999) The premixture model of turbulent burning to describe lifted jet flames. *Combust. Flame*, **119**, 95.

Byggstoyl, S. and Magnussen, B.F. (1985) A model for flame extinction in turbulent flow. In Bradbury, L.J.S. et al. (Eds.), *Turbulent Shear Flows*, Springer Verlag, Berlin, Vol. 4, pp. 381.

Cabra, R., Myhrvold, T., Chen, J.Y., Dibble, R.W., Karpetis, A.N., and Barlow, R.S. (2002) Simultaneous laser Raman-Rayleigh-LIF measurements and numerical modeling of a lifted turbulent H_2/N_2 jet flame in a vitiated coflow. *Proc. Combust. Instit.*, **29**, 1881.

Caviliere, A. and de Joannon, M. (2004) Mild combustion. *Prog. Energy Combust. Sci.*, **30**(4), 329.

Solver manual version 5.6, Ansys Europe, Oxfordshire, UK. (2003).

Cha, M.S. and Chung, S.H. (1996) Characteristics of lifted flames in non-premixed turbulent confined jets. *Proc. Combust. Instit.*, **26**, 121.

Chen, Y.C. and Bilger, R.W. (2000) Stabilization mechanisms of lifted laminar flames in axisymmetric jet flows. *Combust. Flame*, **123**, 23.

Christo, F.C. and Dally, B.B. (2005) Modeling turbulent reacting jets issuing into a hot and diluted coflow. *Combust. Flame*, **142**, 117–129

Coelho, P.J. and Peters, N. (2001) Numerical simulations of a mild combustion burner. *Combust. Flame*, **123**, 503.

Dally, B.B., Riesmeier, E., and Peters, N. (2004) Effect of the fuel mixture on moderate and intense low oxygen dilution combustion. *Combust. Flame*, **137**, 418.

Chakraborthy, D. (1998) Confined Reacting Supersonic Mixing Layer-A DNS Study with Analysis of Turbulence and Combustion Models, Ph.D. thesis, Indian Institute of Science, Bangalore, India.

Domingo, P. and Vervisch, L. (1996) Triple flames and partially premixed combustion in autoignition of non-premixed turbulent mixtures. *Proc. Combust. Instit.*, **26**, 233.

Donnerhack, S. and Peters, N. (1984) Stabilization heights in the lifted methane-air jet diffusion flames diluted with nitrogen. *Combust. Sci. Tech.*, **41**, 101.

Filatyev, S.A., Driscoll, J.F., Carter, C.D., and Donbar, J.M. (2005) A database of turbulent premixed flame properties for model assessment including burning velocities, stretch rates and surface densities. *Combust. Flame*, **141**, 1.

Horch, K. (1978) Zur Stabilitat von Freistrahl-Diffsionsflammen, Ph.D. thesis, University of Karlsruhe.

Kalghatgi, G.T. (1984) Liftoff heights and visible lengths of vertical turbulent jet diffusion flames in still air. *Combust Sci. Tech.*, **41**, 17.

Kumar, S. (2004) Computational and Experimental Studies on Flameless Combustion of Gaseous Fuels, Ph.D. thesis, Indian Institute of Science, Bangalore, India.

Kumar, S., Paul, P.J., and Mukunda, H.S. (2002) Studies on a high intensity low emission burner. *Proc. Combust. Instit.*, **29**, 1131.

Kumar, S., Paul, P.J., and Mukunda, H.S. (2005) Investigation of the scaling criteria for a mild combustion burner. *Proc. Combust. Instit.*, **30/2**, 2613.

Lille, S., Dobski, T., and Blasiak, W. (2000) Visualization of the fuel jet in conditions of highly preheated air combustion. *J. Prop. Power*, **16**, 595.

Mancini, M., Weber, R., and Bollettini, U. (2002) Predicting NO_x emissions of a burner operated in flameless combustion mode. *Proc. Combust. Instit.*, **29**, 1155.

Maruta, K., Muso, K., Takeda, K., and Niioka, T. (2000) Reaction zone structure in flameless combustion. *Proc. Combust. Instit.*, **28**, 2117.

Miake-Lye, R.C. and Hammer, A.J. (1988) Lifted turbulent jet flames: A stability criterion based on the jet large scale structure. *Proc. Combust. Instit.*, **25**, 817.

Montgomery, C.J., Kaplan, C.R., and Oran, E. (1998) The effect of coflow velocity on a lifted methane-air jet diffusion flame. *Proc. Combust. Instit.*, **27**, 1175.

Muller, C.M., Breitbach, H., and Peters, N. (1994) Partially premixed turbulent flame propagation in the jet diffusion flames. *Proc. Combust. Instit.*, **25**, 1099.

Muniz, L. and Mungal, M.G. (1997) Instantaneous flame stabilization velocities in lifted jet diffusion flames. *Combust. Flame*, **111**, 16.

Peters, N. (1999) The turbulent burning velocity for large scale and small scale turbulence. *J. Fluid Mech.*, **384**, 107.

Peters, N. (2000) Turbulent Combustion, Cambridge University Press, Cambridge, U.K.

Peters, N. and Williams, F.A. (1984) Liftoff characteristics of turbulent jet diffusion flames. *AIAA J.*, **21**, 423.

Pitts, W.M. (1989) Importance of isothermal mixing process to the understanding of liftoff and blow-out of turbulent jet diffusion flames. *Combust. Flame*, **76**, 97.

Pitts, W.M. (1990) Large scale turbulent structures and the stabilization of lifted turbulent jet diffusion flames. *Proc. Combust. Instit.*, **23**, 661.

Plessing, T., Terhoeven, P., Monsour, M.S., and Peters, N. (1998a) An experimental and numerical study of a laminar triple flame. *Combust. Flame*, **115**, 335.

Plessing, T., Peters, N., and Wunning, J.G. (1998b) Lasroptical investigation of highly preheated combustion with strong exhaust gas recirculation. *Proc. Combust. Instit.*, **27**, 3197.

Rokke, N.A., Hustad, J.E., and Sonju, A.K. (1994) A study of partially premixed unconfined propane flames. *Combust. Flame*, **97**, 88.

Ruetsch, G.R., Vervisch, L., and Linan, A. (1995) Effect of heat release rates on triple flame. *Phys. Fluids*, **7**(6), 1447.

Savas, O. and Gollahalli, S.R. (1986) Stability of lifted laminar round gas-jet flame. *J. Fluid Mech.*, **165**, 297.

Schefer, R.W. and Goix, P.J. (1998) Mechanism of flame stabilization in turbulent lifted jet flames. *Combust. Flame*, **112**, 559.

Starner, S., Bilger, R.W., Long, M.B., Frank, J.H., and Marran, D.F. (1997) Scalar dissipation measurements in turbulent jet diffusion flames of air diluted methane and hydrogen. *Combust. Sci. Tech.*, **129**, 141.

Tacke, M.M., Linow, S., Geiss, S., Hassel, E.P., Janicka, J., and Chen, J.Y. (1998) Experimental and numerical study of a highly diluted turbulent diffusion flame close to blowout. *Proc. Combust. Instit.*, **27**, 1139.

Upatneiks, A., Driscoll, J.F., Rasmussen, C.C., and Ceccio, S.L. (2004) Liftoff of turbulent jet diffusion flames–assessment of edge flame and other concepts using cinema–PIV. *Combust. Flame*, **138**, 259.

Vanquickenborne, L. and van Tigglen, A. (1966) The stabilization mechanism of lifted diffusion flames. *Combust. Flame*, **10**, 59.

Watson, K.A., Lyons, K.M., Donbar, J.M., and Carter, C.D. (2000) Simultaneous Rayleigh imaging and CH-PLIF measurements in a lifted jet diffusion flame. *Combust. Flame*, **123**, 252.

Watson, K.A., Lyons, K.M., Donbar, J.M., and Carter, C.D. (2003) On scalar dissipation and partially premixed flame propagation. *Combust. Sci. Tech.*, **175**, 649.

Westbrook, C.K. and Dryer, F.L. (1984) Simplified reaction mechanism for the oxidation of hydrocarbon fuels in flames. *Combust. Sci. Tech.*, **27**, 31.

Williams, F.A. (1985) Combustion Theory, Benjamin and Cummins, Menlo Park, CA.

Wunning, J.A. and Wunning, J.G. (1997) Flameless oxidation to reduce thermal NO_x formation. *Prog. Energy Combust. Sci.*, **23**(12), 81.